Terminal Acetylenes React to Increase Unsaturation in $[(^tBu_2PCH_2SiMe_2)_2N]Re(H)_4$

Oleg V. Ozerov, Lori A. Watson, Maren Pink, Mu-Hyun Baik, and Kenneth G. Caulton*

Department of Chemistry, Indiana University, Bloomington, Indiana 47405

Received July 26, 2004

$(PNP^{tBu})Re(H)_4$, where PNP^{tBu} is $(^tBu_2PCH_2SiMe_2)_2N$, reacts at 23 °C with RC≡CH (R = ^{t}Bu, $SiMe_3$, Ph) to give first H_2 and mirror-symmetric $(PNP^{tBu})ReH_3(CCR)$, then H_2 and C_{2v} symmetric $(PNP^{tBu})Re(CCR)_2$. The diacetylide compounds show temperature-independent paramagnetism and ^{13}C and ^{31}P chemical shifts far beyond their normal values for other $(PNP^{tBu})ReX_n$ compounds. Single-crystal X-ray diffraction shows very similar structures for the cases R = Ph and R = $SiMe_3$, each having an approximately C_{2v} geometry with equivalent acetylides with ∠C−Re−C approximately 108°. No hydride or H_2 ligands are detected in final difference Fourier maps. DFT(B3PW91) calculations give minimum energy geometries of these species, of their products upon adding H_2, and of mechanistically significant analogues $[(H_2PCH_2SiH_2)_2N]ReH_nR'_mH_{2-m}$, with $n = 0, 2$, $m = 1, 2$, and R′ = H or Ph. These calculated geometries, when compared to those from X-ray diffraction, indicate that the isolated compounds have no hydride or H_2 ligands and are thus $(PNP)Re^{III}(CCR)_2$, making them more unsaturated than the reagent $(PNP)Re^{V}(H)_4$ by two electrons. Triplet state geometries of (PNP)ReXY are calculated and analyzed, as are their frontier orbitals.

Introduction

The molecule $(PNP^R)Re(H)_4$ (PNP^R = $(R_2PCH_2SiMe_2)_2N$) is a classical hydride of Re^V, having a π-donor ligand, the amide, which stabilizes the otherwise unsaturated (16 valence electron) metal.[1] We have termed this "operational unsaturation" since the Re/N bond is short enough to indicate multiple bonding, yet this molecule forms a 1:1 adduct with Lewis bases, e.g., PMe_3. Because an associative mechanism is thus available, $(PNP^R)Re(H)_4$ reacts rapidly at and below 23 °C with ethylene.[1] As H ligands are lost in this reaction, the metal is reduced and its reducing power (π-basicity) increases. As a result, ethylene is isomerized into a more π-acidic ligand, ethylidyne (eq 1). With cyclic olefins,[2]

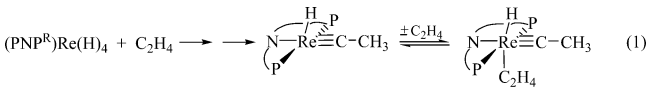

(1)

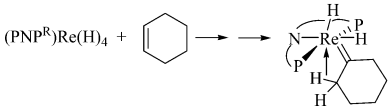

(2)

since the conversion of the unsaturated hydrocarbon cannot effect C−C bond scission (requisite for carbyne formation), the reaction stops at the carbene stage. In one instance, the isomerized olefin, cyclohexene, yields a rare case of a β-agostic carbene (eq 2).

We report here on the distinctly different character of the reaction of $(PNP^{tBu})Re(H)_4$ with terminal alkynes, RC≡CH, which might have been envisioned as candidates for forming a π-acidic vinylidene ligand, Re=C=CHR, but instead form acetylide complexes by loss of H_2.

Results

Synthesis and Characterization. Terminal acetylenes RCCH (R = Ph, $SiMe_3$, and ^{t}Bu) react rapidly with $(PNP^{tBu})Re(H)_4$ in benzene or pentane at 23 °C with immediate gas evolution. ^1H NMR monitoring of the reactions identifies the gas as H_2 and shows no significant amount of the corresponding olefins among the products. The synthetic reaction is thus an acid/base reaction, with H_2 elimination (eq 3). At an alkyne:Re

$$(PNP^{tBu})Re(H)_4 + 2RCCH \rightleftharpoons (PNP^{tBu})Re(CCR)_2 + 3H_2 \quad (3)$$

mole ratio of 3.5:1, the product solution contains two new complexes, blue $(PNP^{tBu})ReH_3(CCR)$ and $(PNP^{tBu})Re(CCR)_2$. At lower mole ratios, the product yields change consistent with $(PNP^{tBu})ReH_3(CCR)$ being an intermediate. Following the time evolution of a reaction with >3:1 alkyne:Re ratio *in a closed system* shows gradual conversion of $(PNP^{tBu})ReH_3(CCR)$ to $(PNP^{tBu})Re(CCR)_2$. The initial (kinetic) product of the reaction of RCCH with $(PNP^{tBu})Re(H)_4$ in benzene or pentane at 23 °C is $(PNP^{tBu})ReH_3(CCR)$. In the presence of more than 1 equiv of RCCH and with removal of H_2, $(PNP^{tBu})ReH_3(CCR)$ is subsequently transformed into $(PNP^{tBu})Re(CCR)_2$. However, even without the extra RCCH present, $(PNP^{tBu})ReH_3(CCR)$ partially disproportionates into $(PNP^{tBu})Re(CCR)_2$ and $(PNP^{tBu})Re(H)_4$. It was

* To whom correspondence should be addressed. E-mail: caulton@indiana.edu.

(1) Ozerov, O. V.; Huffman, J. C.; Watson, L. A.; Caulton, K. G. *Organometallics* **2003**, *22*, 2539.

(2) Ozerov, O. V.; Watson, L. A.; Pink, M.; Caulton, K. G. *J. Am. Chem. Soc.* **2003**, *125*, 9604.

10.1021/om049424i CCC: $27.50
Publication on Web 00/00/0000 PAGE EST: 9.2

independently established that Re−C bond formation is reversible by exposing $(PNP^{tBu})Re(CCPh)_2$ to D_2 at 23 °C. This showed conversion to $(PNP^{tBu})ReD_3(CCPh)$, then $(PNP^{tBu})Re(D)_4$, together with PhCCD.

$(PNP^{tBu})ReH_3(CCR)$ showed a hydride ^1H NMR signal of intensity 3 H (a triplet from coupling to two P) and equivalent phosphorus nuclei. Two P^tBu signals, two $SiMe_2$ signals, and two $SiCH_2$ signals indicate that the hydride fluxionality does not create a time-averaged mirror plane containing the $ReNP_2$ plane; the molecule has only the mirror symmetry defined by the NReCC plane.

$(PNP^{tBu})Re(CCR)_2$ showed unusual NMR spectroscopic behavior (Table 1). While the ^1H and $^{31}P\{^1H\}$ NMR spectra were consistent with C_{2v} symmetry, the ^1H chemical shifts (wholly in the 0−10 ppm region) were significantly (as much as 5 ppm) shifted from their normal[1,2] regions. In addition, the ^{31}P signals, while sharp (half-width ≈ 0.2 ppm at 162 MHz and 23 °C), were shifted to −250 to −400 ppm, while for $(PNP^{tBu})ReH_3(CCR)$, and indeed many $(PNP)ReX_n$ analogues,[1,2] the ^{31}P chemical shifts range from 0 to +85 ppm. These ^{31}P chemical shifts are, moreover, unusually temperature dependent (∼1 ppm/°C). The ^{13}C chemical shifts are also found over a huge range, from −200 to +375 ppm. In contrast, the ^1H NMR of $(PNP^{tBu})Re(CCR)_2$ spectra are not abnormally temperature dependent (changing 0.1 ppm in 18 °C). Both ^1H and ^{13}C lines are sharp and show coupling to ^{31}P.

The earliest observations of strongly temperature-dependent chemical shifts were in ^{59}Co NMR, where changes of 1−3.8 ppm/°C were observed.[3] These were attributed to TIP (better called "second-order paramagnetism"), where the authentically singlet $^1A_{1g}$ ground state of $Co(III)L_6$ was contaminated by mixing in a $^1T_{1g}$ excited state. The temperature dependence of δ was due to temperature-dependent vibrational averaging of this excited state. This orbital angular momentum made a paramagnetic contribution to the magnetic susceptibility χ, despite the purity of spin = zero character.

A select set of Re^{III} and Re^{IV} compounds have a long history of unusual NMR behavior: large ^1H chemical shifts and no ^{31}P NMR signal observable.[4−9] However, the compounds $ReCl_3(PR_2Ph)_3$ and $ReCl_4(PRPh_2)_2$ were never subjected to a careful study of their solid state magnetic susceptibility. We therefore collected SQUID susceptibility data on both species $(PNP^{tBu})Re(CCR)_2$ (R = Ph and $SiMe_3$). The measured susceptibilities of both $(PNP^{tBu})Re(CCR)_2$ are small down to at least 100 K and relatively temperature independent. The plots (see Experimental Section) show that the magnitude of the susceptibility (after correcting for the diamagnetic contribution, by using Pascal's constants) is small compared to the spin-only formula for even one unpaired electron ($\chi_m \cdot T = S(S+1)/2 = 0.375$ cm^3 mol^{-1} for $S = 1/2$). In addition, the observed temperature dependence for two different acetylides can be fit over the full temperature range (see χ_m versus T plots) by assuming <0.8% paramagnetic ($S = {}^1/_2$) impurity, and then the resulting temperature-independent susceptibility is small (consistent with the conclusion above). Indeed, it is on the order of the diamagnetic corrections. The molecules $(PNP^{tBu})Re(CCR)_2$ thus show very small and temperature-independent susceptibilities, and the unusual NMR behavior of these diamagnetic molecules cannot be attributed to unpaired electrons.

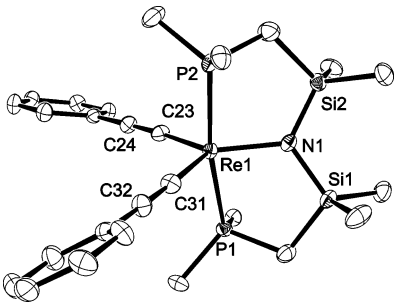

Figure 1. ORTEP drawing (50% probability ellipsoids) of $(PNP^{tBu})Re(CCSiMe_3)_2$, showing selected atom labeling. Crystallographic symmetry element is C_2. Omitted for clarity: all H and the ^{t}Bu methyl groups. Selected structural parameters (Å, deg): Re−C12, 1.980(2); Re−N1, 2.031(2); Re−P1, 2.4392(5); C12−C13, 1.224(3); C12−Re−C12′, 108.75(12); N1−Re−P1′, 85.790(13); P1−Re−P1′, 171.58(3); Re−C12−C13, 176.6(2); N1−Re−C12, 125.62-(6); C12−Re−P1′, 95.11(6); C12′−Re−P1′, 89.79(6).

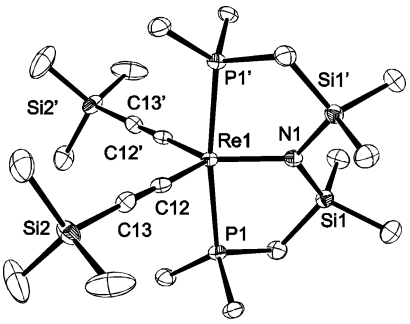

Figure 2. ORTEP drawing (50% probability ellipsoids) of $(PNP^{tBu})Re(CCPh)_2$ showing selected atom labeling. Omitted for clarity: all H and the ^{t}Bu methyl groups. Selected structural parameters (Å, deg): Re−C23, 1.973(2); Re−C31, 1.973(2); Re−N1, 2.0279(18); Re−P1, 2.4369(6); Re−P2, 2.4431(7); C23−C24, 1.228(3); C31−C32, 1.232(4); C23−Re−C31, 108.01(9); N1−Re−P1, 85.28(9); N1−Re−P2, 85.81(9); P1−Re−P2, 170.86(2); Re−C23−C24, 174.6-(2); Re−C31−C32, 176.7(2); N1−Re−C23, 129.15(2), N1−Re−C31, 122.82(15); C23−Re−P1, 88.33(7); C31−Re−P1, 95.93(7), C23−Re−P2, 95.75(7); C31−Re−P2, 90.60(7).

The X-ray structure determination (Figures 1 and 2) shows substantial agreement between the structures of the CCPh and $CCSiMe_3$ analogues. Bond lengths Re−N, Re−P, Re−C, C≡C, and ∠NRe−C show no chemically significant differences between the two. The silyl example has crystallographic C_2 symmetry (the Re−N bond is the C_2 axis), while the phenyl case has only idealized 2-fold symmetry. In neither case were hydrogens detected attached to Re. Negative evidence for hydrides by X-ray diffraction cannot be taken as certain, despite our consistent ability to find and refine hydrides using the SMART 6000 diffractometer. NMR cannot be relied on for the decision here, due to the observation of the unusual magnetism and NMR chemical shifts.

(3) Gielen, M., Willem, R., Wrackmeyer, B., Eds. *Advanced Applications of NMR to Organometallic Chemistry*; Wiley: New York, 1996.
(4) Chatt, J.; Leigh, G. J.; Mingos, D. M. P.; Paske, R. J. *J. Chem. Soc. A* **1968**, 2636.
(5) Leigh, G. J.; Gunz, H. P. *J. Chem. Soc. A* **1971**, 2229.
(6) Shaw, D.; Randall, E. W. *Chem. Commun.* **1965**, 82.
(7) Randall, E. W.; Shaw, D. *Mol. Phys.* **1965**, *10*, 41.
(8) Chatt, J.; Leigh, G. J.; Mingos, D. M. P.; Randall, E. W.; Shaw, D. *Chem. Commun.* **1968**, 419.
(9) Randall, E. W.; Shaw, D. *J. Chem. Soc. A* **1969**, 2867.

Table 1. Temperature Dependence of ^{31}P NMR Chemical Shifts

temp, °C	(PNP^{t}Bu)Re(C≡CSiMe$_3$)$_2$	(PNP^{t}Bu)Re(C≡CPh)$_2$
−40	−277.7	
0		−253.6
10	−340.4	−262.2
20	−354.4	−271.6
21.7	−355.6	−272.6
30	−369.5	−281.1
40	−384.7	−290.8
50	−400.2	−300.9
60	−416.1	−311.3

Multiple efforts at growing the larger crystals required for a neutron diffraction structure determination were unsuccessful. Thus, comparison of the experimental non-hydrogen atom structure to structures of various stoichiometries determined by DFT(B3PW91) geometry optimization might be useful. This use of DFT geometries for "quantitative and qualitative analysis" has been recently demonstrated for the FeMoCo enzyme center,[10−13] and our approach is in the same spirit.

DFT Geometry Optimizations for Singlet [N(SiH$_2$CH$_2$PH$_2$)$_2$]ReH$_n$R$_m$H$_{2-m}$. Minimum DFT(B3PW91) energy structures were determined for singlet spin states of the title species with R = H, C≡CH, and Ph, and with m = 0, 1, 2 and n = 0, 2. The last variation is intended to probe whether the presence or absence of two H ligands has a detectable influence on the non-hydrogen atom skeleton; this is our intended method of learning whether the X-ray structure can indirectly tell whether these molecules have H ligands. The study of three R groups is intended to probe how robust our conclusions are to variation among three different one-electron donor ligands.

The starting geometries for DFT energy minimization for n = 2 in every case (X, Y = R, H) involved nonbonding H/H distances (i.e., >1.3 Å) and all ligands in the same plane, **I**, that are perpendicular to the PNP plane. As will be seen, this involves considerable "migration" of the 2 H (i.e., to the PNP plane), to get to the most stable geometry, and it is unbiased with regard to hydride versus H$_2$ final geometry.

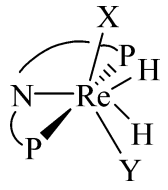

I

The results in Table 2 show the following.

(a) Re−P distances are invariant (±0.01 Å) as are the acetylide C≡C distances (±0.01 Å).

(b) The ground state geometries for n = 2 have a dihydrogen (intact H$_2$) ligand for one or two acetylide ligands (m = 1, 2), but are dihydride complexes (Re^V) for one or two phenyl ligands, and also for R = H. The difference is an H/H distance of 0.90−0.99 Å versus 1.46−1.53 Å. That is, H and phenyl ligands make the metal more reducing than acetylide. We suggest that this distinction arises because acetylide is less of a σ-donor to the metal than either H or Ph; superficially, acetylide is more of a pseudohalide than it is a pure σ-donor like H or phenyl. The orbital explanation is that the larger s component of the sp hybrid orbital in acetylide compared to the sp^2 and sp^3 orbitals of the phenyl and methyl groups gives rise to a notably lower orbital energy for the acetylide than the other two ligands. Therefore, the acetylide is a weaker σ-donor than the phenyl group. Thus, the main distinction between acetylide and methyl or phenyl as a ligand can be traced to the energy of the σ-orbital that will form the M−C bond, and these are shown in Figure 3. Illustrated are the singly occupied orbitals of the radical species C$_6$H$_5$, CH$_3$, and CCH, but calculated at the frozen geometry of the corresponding molecular species H−R. The species CCH has a σ-orbital with an energy of −10.72 eV, which is notably lower than the corresponding orbitals of CH$_3$ or C$_6$H$_5$, at −7.02 and −6.90 eV, respectively. The relatively low orbital energy of the acetylide increases the orbital energy difference from the σ-accepting d-orbital of the metal center, with the consequence that there will be much less mixing of d with the CCH σ-orbital. All three orbitals are drawn to scale in Figure 3, and the larger s component of the acetylide can be readily recognized by comparing the shapes of the orbitals. An additional contributing factor favoring an intact H$_2$ co-ligand may be that acetylide is more π-acidic than the other R groups studied.

(c) Regardless of dihydride or dihydrogen structures, the case n = 2 has an angle between the two R ligands

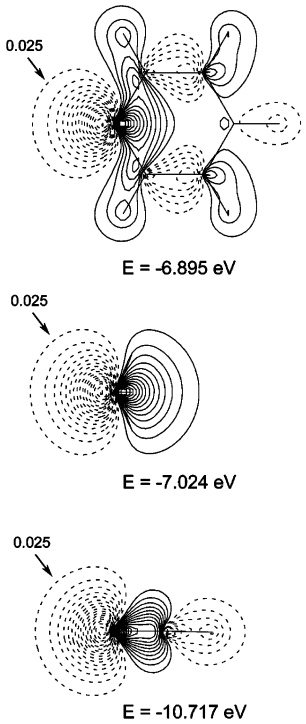

Figure 3. SOMO orbital contour diagrams and energies for phenyl, methyl (middle), and ethynyl (lower) radicals (DFT (B3LYP/6-31G**)/unrestricted) at the fixed geometry of their H−R analogues. Contours are drawn at 0.025 au intervals, and the outmost contour is 0.025, as indicated. All three plots are drawn to scale.

(10) Huniar, U.; Ahlrichs, R.; Coucouvanis, D. *J. Am. Chem. Soc.* **2004**, *126*, 2588.
(11) Hinnemann, B.; Norskov, J. K. *J. Am. Chem. Soc.* **2003**, *125*, 1466.
(12) Dance, I. *Chem. Commun.* **2003**, 324.
(13) Lovell, T.; Liu, T.; Case, D. A.; Noodleman, L. *J. Am. Chem. Soc.* **2003**, *125*, 8377.

Table 2. Structural Parameters for $(PNP^H)ReH_nR_mH_{2-m}$ from DFT Optimization

	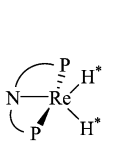	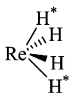	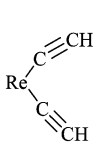	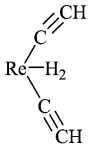			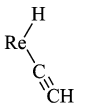	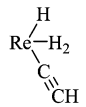		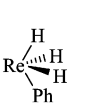
H-H	–	1.525	–	0.90	–	1.46	–	0.99	–	1.46
Re-N	1.979 Å	2.062	1.995	1.999	2.000	2.072	1.986	2.016	1.990	2.069
Re-P	2.342	2.374	2.363	2.376	2.360	2.385	2.353	2.371	2.354	2.382
Re-C1(H^*)	1.667	1.639	1.983	2.044	2.055	2.113	1.666	1.669	1.663	1.643
Re-C2(H^*)	1.663	1.645	1.983	2.050	2.054	2.114	1.978	2.034	2.037	2.102
∠C1(H^*)-Re-C2(H^*)	125.4°	127.7	119.5	149.0	120.4	140.8	121.2	141.0	121.0	135.6
$C_\alpha \equiv C_\beta$	–	–	1.231	1.226	–	–	1.232	1.226	–	–

Table 3. Comparison of Calculated (DFT) and X-ray-Determined Structural Parameters for $(PNP)ReH_n(CCR)_2$

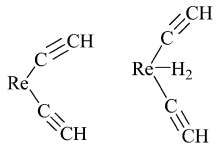

	singlet	triplet	singlet	X-ray
Re-N	1.995	2.064	1.999	2.03 Å
Re-P	2.363	2.406	2.376	2.44
Re-C1	1.983	1.975	2.044	1.97
Re-C2	1.983	1.961	2.050	
$C_\alpha \equiv C_\beta$	1.231	1.235	1.226	1.23
	1.231	1.240	1.226	
∠C-Re-C	119.5°	94.5°	149.0°	108°

larger by 15−30° than for $n = 0$. Predictably, the smaller of these two numbers is for dihydride and the larger is for dihydrogen, because the "bulk" of H_2 lies closer to the C−Re−C plane.

(d) Going from $n = 0$ to $n = 2$, the Re−N distance is longer by 0.07 Å for dihydride ground states, but it lengthens by less than 0.03 Å for a dihydrogen ground state.

Exploring the Paramagnetic Alternative. We also calculated $[(H_2PSiH_2CH_2)_2N]Re(CCH)_2$ in its lowest energy triplet state. Geometries of singlet and triplet are compared in Table 3 and Figure 4. These show the following.

(a) Re−C and C≡C distances are nearly invariant to spin state.

(b) Re−P lengthens by 0.04 Å and Re−N lengthens by 0.07 Å in the triplet, suggesting that the LUMO of the singlet is antibonding in both Re−P and Re−N bonds. Figure 5 confirms this.

(c) The C−Re−C angle is 120° in the singlet but only a very small 94.5° in the triplet. This is consistent with avoidance by carbon of the singly occupied N_π-d_π orbital in the triplet. The triplet state is calculated to lie 13.3 kcal/mol higher than the singlet, which is consistent with the measured magnetic susceptibilities.

Final Conclusion on H Ligands. The data collected in Table 3 compare the DFT-calculated structural parameters for $n = 0$ (singlet and triplet) and for $n = 2$ to the X-ray values. We choose to put the greatest reliance on the angular location of the acetylide C_α (i.e., ∠C−Re−C), and by this criterion the composition with no H on Re (i.e., consistent with the absence of such electron density in the final X-ray Fourier maps) is clearly preferred.

Other Triplet States. To understand the influence of the anionic ligands X and Y on the singlet/triplet energy gap among $(PNP^H)ReXY$ species, we have calculated minimum triplet energy structures for $(PNP^H)Re(H)_2$ and $(PNP^H)ReH(CCH)$, to compare to $(PNP^H)Re(CCH)_2$. These three are compared in Figure 4, together with their energies relative to their singlet states in their minimum energy geometries. In every case, the singlet is more stable, and the singlet−triplet energy gap shows no consistent trend. In each case, the triplet state has the longer Re−N distance and the smaller ∠X−Re−Y, the latter generally near 90°. For $(PNP^H)Re(H)(CCH)$, the structure begins to resemble a

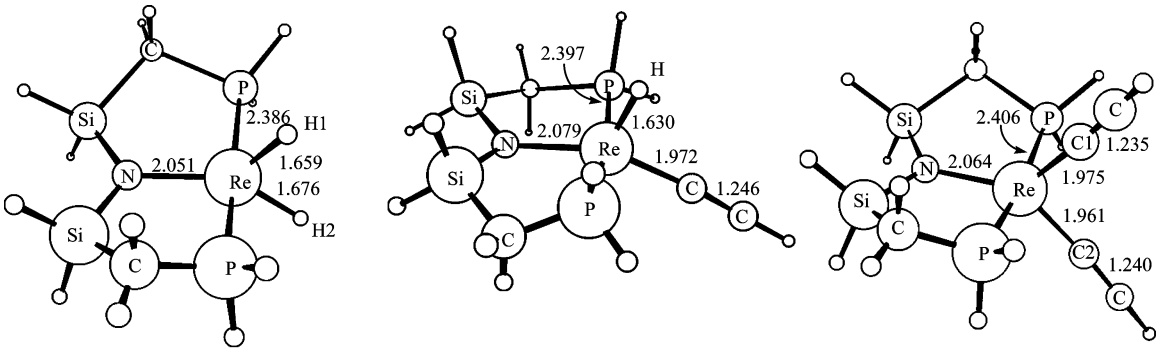

H1-Re-H2: 90.4
N-Re-H1: 130.5
N-Re-H2: 139.1

H-Re-C: 90.8
N-Re-H: 115.1
N-Re-C1: 154.2

C1-Re-C2: 94.5
N-Re-C1: 129.0
N-Re-C2: 136.5

E (kcal/mol): +11.9 +9.3 +13.3

Figure 4. DFT minimum energy geometries for triplet states of species shown, together with their energy relative to the corresponding singlet.

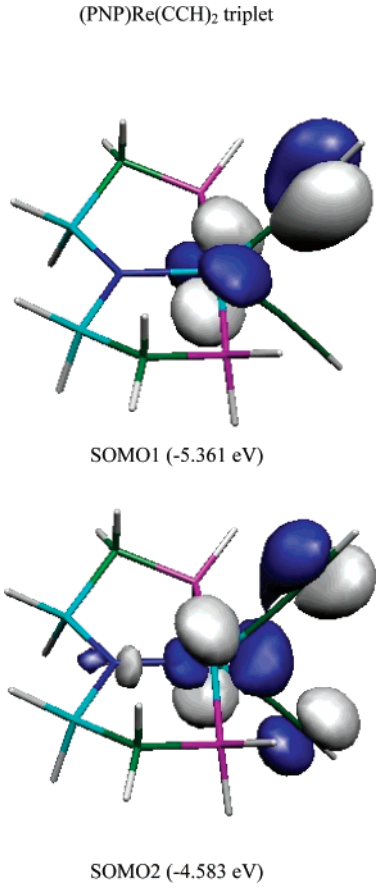

Figure 5. Orbital isosurface plots of the two singly occupied MOs of triplet (PNP^H)Re(CCH)$_2$.

square pyramid, where ∠N−Re−C is 154.2°. In sum, all these Re^{III} species are predicted to be more stable as singlets and with a near 90° X−Re−Y angle.

Discussion

The synthetic reaction employed gives a product whose valence electron count has decreased by two. The reaction transforms Re^V to Re^{III}, a d^4 species. Why is the triplet state only 13 kcal/mol above the singlet? One possible answer is that, even if the coordinated amide nitrogen involves its lone pair in π donation to unsaturated Re, the result is a 16-electron species. Numerous examples have shown[14−18] that, for the early and middle transition metals, it can occasionally be preferable to "save" the spin pairing energy and half fill two frontier orbitals rather than doubly occupy one and leave a small HOMO/LUMO gap (the 18e rule generally promises a small gap for the singlet state of a 16-electron species).[19−21]

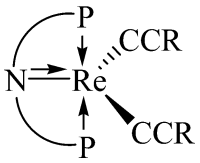

This general answer can be supplemented by one that is specific to an ReX$_3$(PR$_3$)$_2$ case. We begin by noting that Re(Ph)$_3$(PEt$_2$Ph)$_2$ is an authentic 14 valence electron molecule and is diamagnetic.[22,23] To see how the change from one phenyl to one amide can influence the ground spin state, analysis of the relevant d-orbital splitting diagram is helpful. Contrasted below are the d-orbital splitting for D_{3h} RePh$_3$(PR$_3$)$_2$ and C_{2v} (PNP)-Re(CCR)$_2$, both in the same axis system. The key

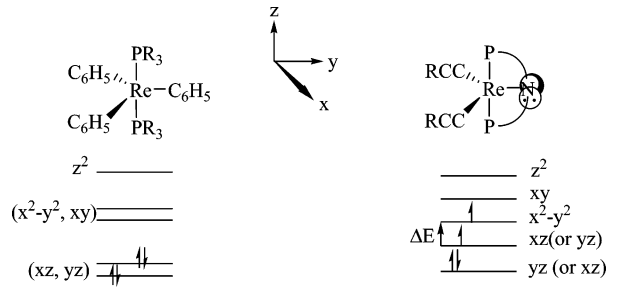

difference is that symmetry reduction to C_{2v} and the change to more halide-like ligands split the two d-orbital degeneracies of D_{3h}, and with more independent energy levels, a small energy gap ΔE becomes possible, when the electronic character of the X ligand is right. The triplet state can then become energetically competitive. The amide nitrogen lone pair (illustrated) does not have the symmetry to mix with any of the three lowest frontier orbitals depicted for (PNP)Re(CCR)$_2$, and so *xy*, which is π^*_{ReN}, remains empty; N → Re π donation is thus unimpaired, to first order, by going from singlet to triplet states.

Reaction Energies (DFT) for Potential Reaction Intermediates. The species described above, together with additional ones, were located at DFT-optimized geometries to establish energetically viable intermediates in the synthesis of (PNP^{tBu})Re(CCR)$_2$. Since these are all energy minima, this view of the potential energy surface alone cannot fully define the mechanism; transition states were not calculated, in part because of the large number of minima considered. Nevertheless, species whose energy is very high make a mechanism passing through that intermediate too slow; the DFT energies can thus help to exclude certain mechanisms. In addition, a high reaction energy is informative since it indicates some destabilizing features of that product. As such, this permits better understanding of the bonding potential of the [(R$_2$PCH$_2$SiMe$_2$)$_2$N]Re substructure: its reducing power, the influence of changing metal oxidation state, trans effect, and the character (bonding or antibonding) of certain frontier orbitals.

(a) Acetylides. Scheme 1 shows reaction energies (ΔE + ZPE differs only insignificantly from enthalpies)

(14) Harvey, J. N.; Poli, R.; Smith, K. M. *Coord. Chem. Rev.* **2003**, *238−239*, 347.
(15) Smith, K. M.; Poli, R.; Harvey, J. N. *New J. Chem.* **2000**, *24*, 77.
(16) Poli, R. *Acc. Chem. Res.* **1997**, *30*, 494.
(17) Poli, R. *Comments Inorg. Chem.* **1992**, *12*, 285.
(18) Abugideiri, F.; Keogh, D. W.; Poli, R. *J. Chem. Soc., Chem. Commun.* **1994**, 2317.
(19) Hessen, B.; Teuben, J. H.; Lemmen, T. H.; Huffman, J. C.; Caulton, K. G. *Organometallics* **1985**, *4*, 946.
(20) Hessen, B.; Lemmen, T. H.; Luttikhedde, H. J. G.; Teuben, J. H.; Petersen, J. L.; Huffman, J. C.; Jagner, S.; Caulton, K. G. *Organometallics* **1987**, *6*, 2354.
(21) Hessen, B.; Meetsma, A.; Teuben, J. H. *J. Am. Chem. Soc.* **1988**, *110*, 4860.
(22) Carroll, W. E.; Bau, R. *J. Chem. Soc., Chem. Commun.* **1978**, 825.
(23) Chatt, J.; Garforth, J. D.; Rowe, G. A. *J. Chem. Soc. A* **1966**, 1834.

Scheme 1[a]

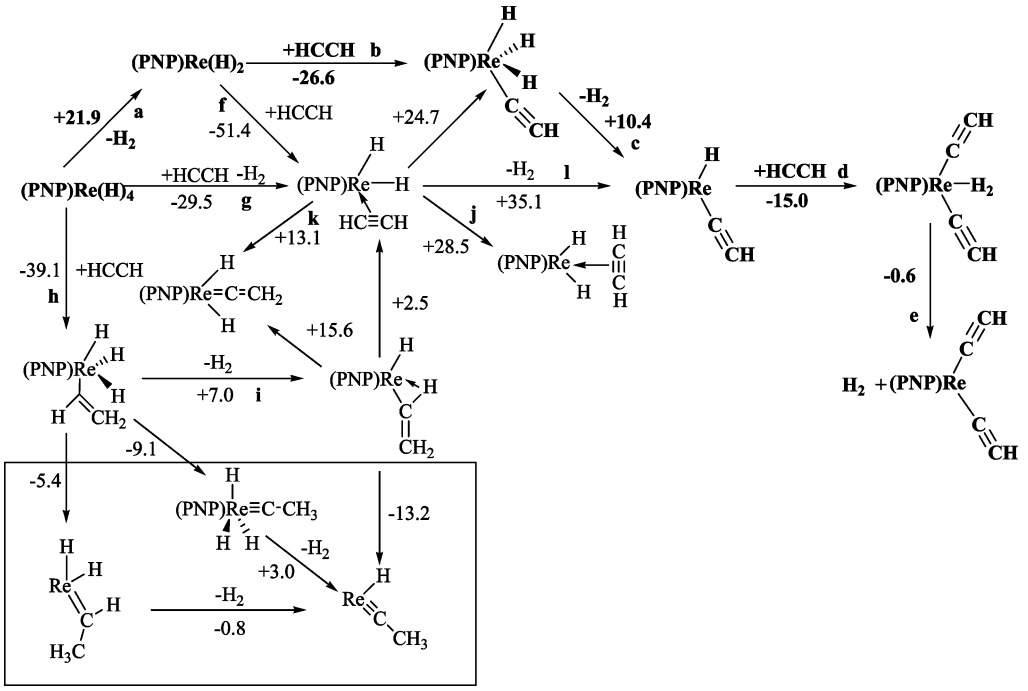

[a] Δ(E + ZPE), kcal/mol.

for various (PNP^H)ReH_n(CCH)$_{1\text{ or }2}$ species, representing the addition of one or two acetylenes and release of various amounts of H_2. An initial loss of H_2, when compensated by $T{\cdot}\Delta S°$ of about 8 kcal/mol,[24,25] characterizes one possible first step, generating the exceptionally reactive (PNP)Re$(H)_2$ (note reaction energy for eq f). However, combining these two into a displacement of H_2 by HCCH gives better energetics (eq g versus a + f). A second possible product of attack of HCCH on intact (PNP)Re$(H)_4$ is h, with a very favorable reaction energy to give the η^1-vinyl complex. H_2 is only weakly bound in this species (BDE 7.0 kcal/mol, which will be compensated by 8 kcal/mol $T{\cdot}\Delta$S), so one rapidly forms the α-agostic monohydride (eq i**)**, which is only slightly more stable than (PNP)Re$(H)_2$(HCCH). The energies of two isomers of this η^2-HCCH species, a structural isomer (eq j, 28.5 kcal/mol higher) and a redox isomer (eq k, 13.1 kcal/mol higher), show that (PNP)Re$(H)_2$(HCCH) lies in a remarkably deep energy well, such that it might reach an experimentally detectable concentration if it were kinetically accessible. Its stability is also reflected in the unreasonably large (versus experiment) positive reaction energy, +35.1 kcal/mol, to lose H_2 and form an acetylide, eq l. Thus, an attractive alternative mechanism would be oxidative addition of the C−H bond of HCCH to transient (PNP)Re$(H)_2$ (reaction b, energy −26.6 kcal/mol), followed by loss of H_2 (eq c, +10.4 kcal/mol) to give (PNP)ReH(CCH). Oxidative addition of the C−H of a second molecule of acetylene to this intermediate is favorable (eq d, −15.0 kcal/mol), and the resulting dihydrogen (H_2) complex easily (eq e, −0.6 kcal/mol) loses H_2 to give the observed product. The energy of this last reaction clearly confirms our aggregate conclusion from above that the isolated reaction product from HCCPh or HCCSiMe_3 contains no H ligands on Re.

It also bears mention that any reaction could be made 47.1 kcal/mol more favorable (E + ZPE) by the addition of hydrogenation of 1 mol of HCCH. Either this could benefit a reaction shown as "$-H_2$", or it could consume 2H from an ReH_2 substructure currently shown in Scheme 1 as persisting throughout the reaction. It should also be noted that the use of H in the DFT calculations fails to model steric effects. Therefore, energies of associative and of dissociative steps involve errors, but of predictable character.

(b) Phenyls. For comparison of H, C_6H_5, and CCH as substituents on such a conversion of (PNP)Re$(H)_4$ to (PNP)Re$H_nR_mH_{2-m}$, Scheme 2 shows transformations related to Scheme 1. Analogous reactions are shown with the same letter label plus a prime symbol. All of the species not shown in bold in Scheme 1 are of course absent in Scheme 2. The reaction energies in Scheme 2 show that Re−H and Ph−H are thermodynamically better than Re−Ph and H−H to a similar extent for Re$(H)_4$ (eq x′, +9.7 kcal/mol) and Re$(H)_3$Ph (eq y′, +10.5 kcal/mol) as test cases; there is thus no major consequence for σ-bond metathesis thermodynamics of phenyl versus H as "spectator" substituent on Re. On the other hand (eq a′ versus eq c′ or e′) H_2 binds much stronger to Re$(H)_2$ than to Re(H)Ph or Re$(Ph)_2$. The higher reactivity of H−CCH compared to H−Ph is also evident in the more favorable Δ(E + ZPE) for reactions with Re$(H)_2$ (b versus b′) and ReH(Ph) (d versus d′). A compensating reflection of the reactivity of Re$(H)_2$ versus Re(H)(Ph) is that oxidative addition of benzene to the former (eq b′, −12.2 kcal/mol) is much more favorable than to the latter (eq d′, −0.4 kcal/mol). As a result, while an associative path for eq x′ is preferred for H−Ph oxidative addition to Re$(H)_4$, it is not (eq y′ versus c′) for benzene oxidative addition to Re$(H)_3$Ph.

(24) Watson, L. A.; Eisenstein, O. *J. Chem. Educ.* **2001**, *79*, 1269.
(25) Minas de Piedade, M. E.; Martinho Simoes, J. A. *J. Organomet. Chem.* **1996**, *518*, 167.

Scheme 2[a]

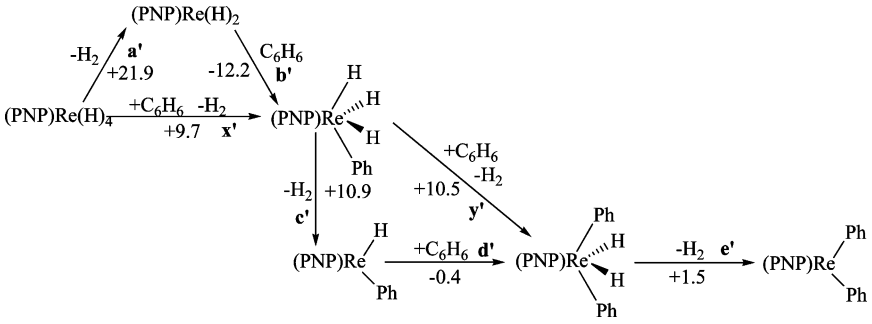

[a] $\Delta(E + ZPE)$, kcal/mol.

Finally (eq e′), binding of H_2 to (PNP)Re(Ph)$_2$ (1.5 kcal/mol) is insignificantly strong, just as it was to (PNP)Re(H)$_2$(CCH)$_2$. Regarding structure, neither the (PNP)ReH(Ph) nor the (PNP)Re(Ph)$_2$ species is *ortho*-agostic to the unsaturated metal.

Mechanistic Speculation. The low activation energy suggested by the rapid reaction of (PNP^{tBu})Re(H)$_4$ with RCCH at 23 °C rules out preliminary H_2 loss from the Re reagent (a in Scheme 1). The large steric bulk of the (PNP^{tBu}) ligand probably favors products (and intermediates) of smaller steric profile. This may contribute to the preference for the observed σ-alkynyl products and intermediates as opposed to the η^2-alkyne complexes because the reagent complex is very crowded. We therefore favor an acid/base reaction (eq 4), which immediately evolves H_2. The intermediates (PNP^{tBu})-

$$(PNP^{tBu})Re(H)_4 + RCCH^* \rightarrow (PNP^{tBu})Re(H)_3(CCR) + H{-}H^* \quad (4)$$

Re(H)$_3$(CCR) were detected for R = Ph, SiMe$_3$, and ^{t}-Bu, and these diamagnetic species have had their hydride content quantitated by ^{1}H NMR integration and quartet splitting in the selectively hydride-coupled ^{31}P NMR spectrum. If indeed the acidity of RCCH is the origin of the first mechanistic step, it is clear why the reaction does not go in the direction of vinyl, vinylidene, or carbyne products shown in Scheme 1. In this regard, olefins convert (PNP^{tBu})Re(H)$_4$ to a hydrido carbyne species.[1] The mild conditions employed also enable kinetic control; the migration of hydrogen from M or from C$_\alpha$ in η^1-vinyl complexes has been generally found[26,27] to involve a high (>30 kcal/mol) barrier. Experimentally, when this acid/base mechanism is eliminated, so too is the rapid reaction: benzene does not compete with RCCH in reaction with (PNP^{tBu})Re(H)$_4$ because the acid/base mechanism is not relevant for arenes. Exchange of (PNP^{tBu})Re(H)$_4$ hydrides with C$_6$D$_6$ (neat) is not detectable over 3 h at 23 °C, and no phenyl complexes accumulate, consistent with the reaction energies in Scheme 2.

It is also relevant that we observe at most 10% of hydrogenated alkyne as product, and we *do* observe either free H_2 or products that put H on Re. The steps in Scheme 1 involving H_2 evolution are thus the most relevant. At the same time, we demonstrated experimentally (via reaction with H_2 or D_2) that hydrogen converts (PNP^{tBu})Re(CCR)$_2$ back to (PNP^{tBu})ReH$_3$(CCR), then to (PNP^{tBu})Re(H)$_4$, making vacuum removal of H_2 an effective way to drive the reaction fully to (PNP^{tBu})-Re(CCR)$_2$. During this (slow) hydrogenolysis reaction, there is no evidence (>1%) of H_2 coordinating to, or even broadening the NMR signals of, (PNP^{tBu})Re(CCR)$_2$.

Conclusions. The reason for the title conclusion is the weak binding of H_2 to either of the (PNP)ReR$_2$ species discussed here (R = CCR′ or Ph). This contrasts with the case of R = H (Scheme 1) and illustrates the fundamental reluctance of unsaturated polyhydrides to form, and thus the high reactivity, once formed, of unsaturated polyhydrides (e.g., (PNP)Re(H)$_2$). Finally, Scheme 1 shows clearly that the most thermodynamically stable product of a 1:1 reaction of (PNP)Re(H)$_4$ and HCCH is (PNP)ReH(≡C−CH$_3$) (cf. eq 5), and thus the observed product is the result of *kinetic control*. In fact, the two unimolecular H migration reactions shown in the box in Scheme 1, have both been shown[28,29] to have high barriers, and these are likely the steps that effect kinetic control in the experiments reported here.

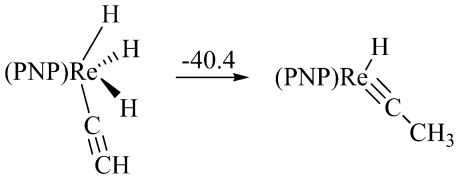

(5)

Integrating the several observations and the DFT computations on (PNP^{tBu})Re(CCR)$_2$ species, these appear to have essentially diamagnetic ground states but with very minor mixing of an excited state into the ground state wave function, together with vibrational averaging, which leads to the anomalous NMR behavior: unusually large ^{13}C and ^{31}P chemical shifts (these nuclei being closer to the metal center) that show large temperature dependence (^{31}P), concurrent with relatively ordinary and temperature-insensitive ^{1}H NMR chemical shifts. It remains to be seen whether Re(III) and Os(IV) are the only metals in which these effects manifest themselves, or whether selected d^4 species of other metals will also show these phenomena. It is worth noting that the cases reported here have a different coordination number than the previous ReCl$_3$L$_3$ and OsCl$_4$L$_2$ examples, so octahedral geometry is not demanded.

(26) Ipaktschi, J.; Mohsseni-ala, J.; Uhlig, S. *Eur. J. Chem.* **2003**, 4313.
(27) Perez-Carreno, E.; Paoli, P.; Ienco, A.; Mealli, C. *Eur. J. Chem.* **1999**, 1315.
(28) Dolker, N.; Frenking, G. *J. Organomet. Chem.* **2001**, *617−618*, 225.
(29) Stegmann, R.; Frenking, G. *Organometallics* **1998**, *17*, 2089.

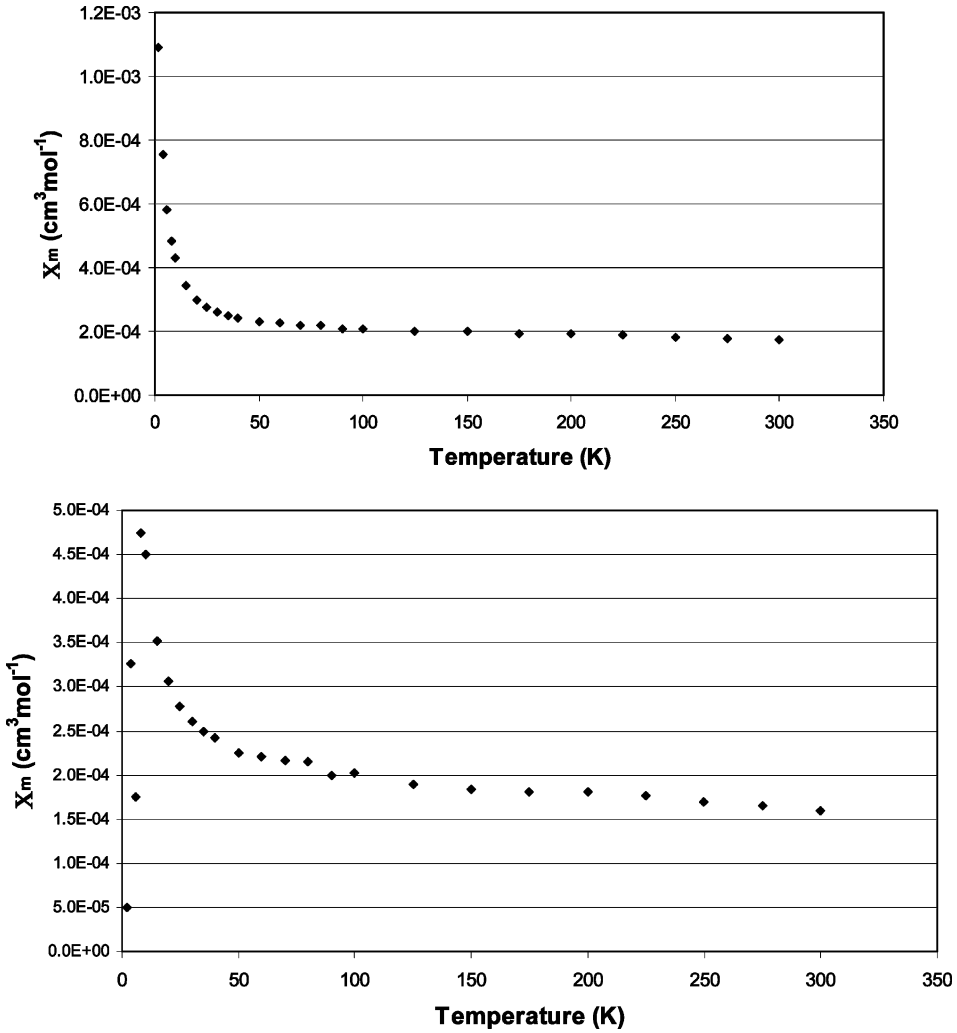

Figure 6. Plots of magnetic susceptibility of $(PNP^{tBu})Re(CCR)_2$ for R = Ph (above) and R = $SiMe_3$ (below).

The products with unusual magnetic and especially NMR behavior here are those with low coordination number, 5, in $(PNP^{tBu})Re(CCR)_2$. In general, low coordination number causes less splitting of the five d-orbitals, and thus other spin states can become competitive with the singlet. It can sometimes become preferable to half fill orbitals when the sub-18 electron count would leave an orbital completely empty, thus apparently contributing nothing to species stability. It is also relevant that the unusual magnetism is observed with the acetylide ligand, which our analysis has shown is the weakest sigma donor, the most halide-like (cf. "weak-field" ligands). The unusal NMR phenomena represent additional evidence that the product is Re(III) and thus argue against the presence of undetected hydride ligands.

Experimental Section

General Considerations. All manipulations were performed using standard Schlenk techniques or in an argon-filled glovebox unless otherwise noted. Pentane, *n*-hexane, C_6D_6, and C_7D_8 were vacuum transferred from NaK/benzophenone/18-crown-6. Alkynes were stirred over and then vacuum transferred from CaH_2. $(PNP^{tBu})Re(H)_4$ was prepared as reported elsewhere.[1] ^{1}H NMR chemical shifts are reported in ppm relative to protio impurities in the deuterated solvents. ^{31}P spectra are referenced to external standards of 85% H_3PO_4 (at 0 ppm). NMR spectra were recorded with a Varian Gemini 2000 (300 MHz ^{1}H; 121 MHz ^{31}P; 75 MHz ^{13}C), a Varian Unity Inova instrument (400 MHz ^{1}H; 162 MHz ^{31}P; 101 MHz ^{13}C), or a Varian Unity Inova instrument (500 MHz ^{1}H; 126 MHz ^{13}C). Elemental analyses were performed by CALI, Inc. (Parsippany, NJ). ORTEP plots were generated using Ortep-3 for Windows.[30]

Magnetic Measurements. Magnetic measurements were performed on a Quantum Design MPMS-XL SQUID magnetometer equipped with a 70 kG (7 T) magnet. Direct current susceptibility data were collected on powdered microcrystalline samples contained in evacuated, sealed NMR tubes, using a field of 1 kG (0.1 T) in the 300−306 K temperature range. Pascal's constants were used to estimate the diamagnetic correction for the complex, which was then applied to the experimental susceptibility to give the molar paramagnetic susceptibility (χ_M), Figure 6. The *different* susceptibility behavior for different R below 10 K suggests that this is not an intrinsic property of $(PNP^{tBu})Re(CCR)_2$, but instead an impurity-derived phenomenon.

Attempts to fit the temperature dependence of the ^{31}P chemical shifts show (Supporting Information) that a δ versus T fit is modestly better than a δ versus $1/T$ plot. We also considered a singlet ground state (chemical shift δ_S) in thermal equilibrium with a triplet state (δ_T) lying higher by $\Delta G°$. The average chemical shift of such a system is given by

$$\delta_{av} = \frac{\delta_S}{1 + e^{-\Delta G°/RT}} + \frac{\delta_T}{1 + e^{-\Delta G°/RT}}$$

We modeled the temperature dependence of δ (^{31}P) for different

assumed values of δ_T, the (unknown) chemical shift of the (unobservably broad) triplet species: -10^2, -10^3, and -10^4 ppm (see Supporting Information). For a $\Delta G°$ value equal to the singlet/triplet difference calculated by DFT, the variation of δ is extremely small, even for $\delta_T = -10^4$. For a smaller $\Delta G°$, δ changes more, but the population of the triplet becomes large enough that varying line broadening should be seen in the averaged signal, contradicting experiment.

(PNP^{tBu})Re(C≡CPh)$_2$. (PNP^{tBu})Re(H)$_4$ (125 mg, 193 μmol) was dissolved in 5 mL of pentane, and PhC≡CH (85 μL, 772 μmol) was added to it. This caused rapid gas evolution and change of color to deep blue. The mixture was stirred while being periodically exposed to vacuum for 10−15 s periods, until most of the volatiles were removed. Then another 5 mL of pentane was added and the slow removal of volatiles was repeated. The purplish brown residue was dissolved in a minimal amount of pentane and placed into a −30 °C freezer overnight. The next day the brownish crystalline product was separated by decantation, washed with cold pentane, and dried in vacuo. Yield: 115 mg (70%). The supernatant contained only the product (besides solvent and traces of phenylacetylene).

^{1}H NMR (C_7D_8, 22 °C): δ 8.64 (t, 8 Hz, 4H, *m*-Ph), 2.91 (d, 8 Hz, 4H, *o*-Ph), 2.31 (t, 8 Hz, 2H, *p*-Ph), 2.16 (t, $J_{HP} = 5$ Hz, 36H, PC(C*H*$_3$)$_3$), 2.01 (br s, 4H, PC*H*$_2$Si), 0.23 (s, 12H, SiC*H*$_3$). ^{31}P{^{1}H} NMR (C_7D_8, 21.7 °C): δ −272.6 (s). ^{13}C{^{1}H} NMR (C_7D_8, 22 °C): δ 374.6, 200.1, 147.5, 116.2, 57.4 (t, 7 Hz), 44.2, 41.5, 32.8, 15.1, −140.8 (m). Anal. ($C_{24}H_{51}N_2P_2ReSi_2$) Calcd (Found): C, 54.51 (54.37); H, 7.46 (7.65); N, 1.67 (1.66).

^{1}H NMR (C_7D_8, +**40 °C**): δ 8.75 (t, 8 Hz, 4H, *m*-Ph), 2.60 (d, 8 Hz, 4H, *o*-Ph), 2.03 (t, 8 Hz, 2H, *p*-Ph), 2.20 (t, $J_{HP} = 6$ Hz, 36H, PC(C*H*$_3$)$_3$), 2.08 (br s, 4H, PC*H*$_2$Si), 0.21 (s, 12H, SiC*H*$_3$).

(PNP^{tBu})Re(C≡CTol)$_2$. (PNP^{tBu})Re(C≡CTol)$_2$ (Tol = *para*-tolyl = C_6H_4Me-*p*) was prepared analogously from (PNP^{tBu})-Re(H)$_4$ (130 mg, 204 μmol) and TolC≡CH (70 mg, 600 μmol). Yield: 130 mg (74%).

^{1}H NMR (C_6D_6, 22 °C): δ 8.56 (d, 8 Hz, 4H, *m*-Tol), 5.85 (s, 6H, Ar-C*H*$_3$), 2.92 (d, 8 Hz, 4H, *o*-Tol), 2.23 (t, $J_{HP} = 5$ Hz, 36H, PC(C*H*$_3$)$_3$), 2.06 (br s, 4H, PC*H*$_2$Si), 0.24 (s, 12H, SiC*H*$_3$). ^{31}P{^{1}H} NMR (C_7D_8, 25 °C): δ −282.4 (s).

(PNP^{tBu})Re(C≡CSiMe$_3$)$_2$. (PNP^{tBu})Re(H)$_4$ (0.50 g, 0.77 mmol) was dissolved in 5 mL of pentane, and Me$_3$SiC≡CH (0.71 mL, 5.0 mmol) was added to it. This caused rapid gas evolution and change of color to deep blue. The mixture was stirred for 2 h while being periodically exposed to vacuum for ca. 1−2 s periods, followed by complete removal of volatiles in vacuo. The residue was treated with Me$_3$SiC≡CH (0.2 mL, 1.4 mmol) and 3 mL of pentane to complete the conversion of hydrides to (PNP^{tBu})Re(CCSiMe$_3$)$_2$. A homogeneous purple solution formed and was stirred for 30 min. Then the volatiles were removed in vacuo, and the residue was dissolved in a minimal amount of *n*-hexane and filtered through a pad of Celite to remove a minute amount of insolubles. Crystallization from *n*-hexane at −30 °C produced highly crystalline material (0.46 g), which was washed with cold *n*-hexane and dried in vacuo. Similar recrystallization from the supernatant gave another 0.11 g of the product. Total yield: 0.57 g (89%). The product is extremely lipophilic. In order for the crystallization to succeed it was found imperative that Me$_3$SiC≡CH be freshly vacuum transferred from CaH_2 and (PNP^{tBu})Re(H)$_4$ be freshly recrystallized.

^{1}H NMR (C_7D_8, 22 °C): δ 2.36 (t, $J_{HP} = 6$ Hz, 36H, PC(C*H*$_3$)$_3$), 2.16 (br t, $J_{HP} = 4$ Hz, 4H, PC*H*$_2$Si), 0.56 (s, 18H, Si(C*H*$_3$)$_3$), 0.14 (s, 12H, Si(C*H*$_3$)$_2$ of PNP). ^{31}P{^{1}H} NMR (C_7D_8, 21.7 °C): δ −355.6 (s). ^{13}C{^{1}H} NMR (C_7D_8, 22 °C): δ 377.1 (s), 62.6 (t, $J = 7$ Hz), 49.4 (s), 39.7 (s), 34.4 (s), 18.3 (s), −201.6 (m). ^{1}H NMR (C_7D_8, −40 °C): δ 2.19 (br s, 36H, PC(C*H*$_3$)$_3$), 1.91 (br s, 4H, PC*H*$_2$Si), 0.50 (s, 18H, Si(C*H*$_3$)$_3$), 0.22 (s, 12H, Si(C*H*$_3$)$_2$ of PNP).

(30) Faruguia, L. J. *J. Appl. Crystallogr.* **1997**, *30*, 565.

NMR Monitoring of Reactions of (PNP^{tBu})Re(H)$_4$ with Terminal Alkynes. General. The reactions of (PNP^{tBu})Re-(H)$_4$ with 1−10 equiv of RC≡CH produced mixtures of (PNP^{tBu})Re(H)$_4$, (PNP^{tBu})ReH$_3$(C≡CR), (PNP^{tBu})Re(C≡CR)$_2$, RC≡CH, and H_2, whose time evolution is described below. These mixtures generally had a navy blue color of (PNP^{tBu})-ReH$_3$(C≡CR). Selectively hydride-*coupled* ^{31}P NMR spectra yielded a quartet, indicating the presence of three H ligands on Re. Initially, (PNP^{tBu})ReH$_3$(C≡CR) was the major component, but over time (at 22 °C in a closed J. Young NMR tube) the fraction of (PNP^{tBu})ReH$_3$(C≡CR) decreased. In all cases a small (<10%) amount of RCH=CH$_2$ was also observed.

(a) (PNP^{tBu})Re(H)$_4$ + Me$_3$SiC≡CH. (PNP^{tBu})Re(H)$_4$ (24.0 mg, 37 μmol) was mixed with Me$_3$SiC≡CH (21.1 μL, 148 μmol) in 0.6 mL of C_6D_6. Integration of the ^{1}H NMR spectrum (20 min after mixing at 22 °C) revealed that the ratio between (PNP^{tBu})Re(C≡CSiMe$_3$)$_2$, (PNP^{tBu})ReH$_3$(C≡CSiMe$_3$), and (PNP^{tBu})Re(H)$_4$ was 10:90:0 (plus excess free Me$_3$SiC≡CH). After 24 h at 22 °C in a closed J. Young tube the ratio changed to 32:68:0. After 48 h, the ratio was 40:60:0. At this time, the solution was degassed by two freeze−pump−thaw cycles. Ten minutes after degassing, the ratio was 77:23:0. Another 24 h later the ratio changed to 87:13:0. The NMR tube was then back-filled with 1 atm of H_2 to test for reversibility of the reaction; 10 min later the ratio was 69:31:0.

Data for (PNP^{tBu})ReH$_3$(C≡CSiMe$_3$). ^{1}H NMR (C_6D_6, 22 °C): δ 1.49 (t, $J_{HP} = 6$ Hz, 18H, PC(C*H*$_3$)$_3$), 1.20 (t, $J_{HP} = 6$ Hz, 18H, PC(C*H*$_3$)$_3$), 1.05 (br dt, 2H, PC*H*$_2$Si), 0.80 (br dt, 2H, PC*H*$_2$Si), 0.35 (s, 6H, SiC*H*$_3$ of PNP), 0.32 (s, 9H, C≡CSi-(C*H*$_3$)$_3$), 0.25 (s, 6H, SiC*H*$_3$ of PNP), −6.33 (br, 3H, Re*H*$_3$). ^{31}P-{^{1}H} NMR (C_6D_6, 22 °C): δ 72.8 (s).

(b) (PNP^{tBu})Re(H)$_4$ + PhC≡CH. (PNP^{tBu})Re(H)$_4$ (24.0 mg, 37 μmol) was mixed with PhC≡CH (4.1 μL, 37 μmol) in 0.6 mL of C_6D_6. Integration of the ^{1}H NMR spectrum (10 min after mixing at 22 °C) revealed that the ratio between (PNP^{tBu})Re-(C≡CPh)$_2$, (PNP^{tBu})ReH$_3$(C≡CPh), and (PNP^{tBu})Re(H)$_4$ was 4:89:7 (plus ca. 10% free PhC≡CH). After 18 h at 22 °C in a closed J. Young tube the ratio changed to 25:37:38, while free PhC≡CH was completely consumed.

Data for (PNP^{tBu})ReH$_3$(C≡CPh). ^{1}H NMR (C_6D_6, 22 °C): δ 7.35 (d, 8 Hz, 2H, *o*-Ph), 7.18 (t, 8 Hz, 2H, *m*-Ph), 6.86 (t, 8 Hz, 1H, *p*-Ph), 1.46 (t, $J_{HP} = 6$ Hz, 18H, PC(C*H*$_3$)$_3$), 1.22 (t, $J_{HP} = 6$ Hz, 18H, PC(C*H*$_3$)$_3$), 1.08 (br dt, 2H, PC*H*$_2$Si), 0.83 (br dt, 2H, PC*H*$_2$Si), 0.39 (s, 6H, SiC*H*$_3$) 0.28 (s, 6H, SiC*H*$_3$), −6.10 (t, $J_{HP} = 24$ Hz, 3H, Re*H*$_3$). ^{31}P{^{1}H} NMR (C_6D_6, 22 °C): δ 72.1 (s).

(c) (PNP^{tBu})Re(H)$_4$ + TolC≡CH. (PNP^{tBu})Re(H)$_4$ (13.0 mg, 20 μmol) was mixed with TolC≡CH (5.1 μL, 40 μmol) in 0.6 mL of C_6D_6. Integration of the ^{1}H NMR spectrum (30 min after mixing at 22 °C) revealed that the ratio between (PNP^{tBu})Re-(C≡CTol)$_2$, (PNP^{tBu})ReH$_3$(C≡CTol), and (PNP^{tBu})Re(H)$_4$ was 22:71:7 (plus some free TolC≡CH).

Data for (PNP^{tBu})ReH$_3$(C≡CTol). ^{1}H NMR (C_6D_6, 22 °C): δ 7.32 (d, 8 Hz, 2H, *m*-Tol), 7.02 (d, 8 Hz, 2H, *o*-Tol), 1.92 (s, 3H, Ar−C*H*$_3$), 1.49 (t, $J_{HP} = 6$ Hz, 18H, PC(C*H*$_3$)$_3$), 1.24 (t, $J_{HP} = 6$ Hz, 18H, PC(C*H*$_3$)$_3$), 1.10 (br dt, 2H, PC*H*$_2$Si), 0.86 (br dt, 2H, PC*H*$_2$Si), 0.40 (s, 6H, SiC*H*$_3$) 0.28 (s, 6H, SiC*H*$_3$), −6.16 (t, $J_{HP} = 24$ Hz, 3H, Re*H*$_3$). ^{31}P{^{1}H} NMR (C_6D_6, 22 °C): δ 71.3 (s).

(d) (PNP^{tBu})Re(H)$_4$ + ^{t}BuC≡CH. (PNP^{tBu})Re(H)$_4$ (24.0 mg, 37 μmol) was mixed with ^{t}BuC≡CH (18.3 μL, 148 μmol) in 0.6 mL of C_6D_6. The mixture was shaken well for 5 min, and then the solution was degassed by two freeze−pump−thaw cycles. Integration of the ^{1}H NMR spectrum of the resulting mixture revealed that the ratio between (PNP^{tBu})Re(C≡CBu^t)$_2$, (PNP^{tBu})-ReH$_3$(C≡CBu^t), and (PNP^{tBu})Re(H)$_4$ was 26:52:22 (plus excess free ^{t}BuC≡CH).

Data for (PNP^{tBu})ReH$_3$(C≡CBu^t). ^{1}H NMR (C_6D_6, 22 °C): δ 1.49 (t, $J_{HP} = 6$ Hz, 18H, PC(C*H*$_3$)$_3$), 1.23 (t, $J_{HP} = 6$ Hz, 18H, PC(C*H*$_3$)$_3$), 0.96 (br dt, 2H, PC*H*$_2$Si), 0.86 (br dt, 2H,

PCH_2Si), 0.35 (s, 6H, SiCH_3) 0.23 (s, 6H, SiCH_3), −6.52 (br, 3H, ReH_3). $^{31}P\{^1H\}$ NMR (C_6D_6, 22 °C): δ 71.6 (s).

Data for (PNP^{tBu})Re(C≡CBu^t)$_2$. ^{1}H NMR (C_6D_6, 22 °C): δ 1.96 (t, J_{HP} = 5 Hz, 36H, PC(CH_3)$_3$), 1.81 (t, 4 Hz, 4H, PCH_2-Si), 1.58 (s, 18H, C≡C−C(CH_3)$_3$), 0.27 (s, 12H, SiCH_3).

Reaction of (PNP^{tBu})Re(C≡CPh)$_2$ with D$_2$. (PNP^{tBu})Re-(C≡CPh)$_2$ (28.0 mg, 33.0 μmol) was dissolved in 0.6 mL of C_6D_6 in a J. Young NMR tube. The solution was degassed and the NMR tube was filled with ca. 300 Torr of D_2 (ca. 2 mL, ca. 35 μmol). The reaction was monitored by ^{1}H NMR. Only traces (<2%) of (PNP^{tBu})ReH_3(C≡CPh) were observed after 10 min. After 24 h ca. 20% of (PNP^{tBu})Re(C≡CPh)$_2$ underwent hydrogenolysis, but *protio* Re−H peaks of (PNP^{tBu})ReH_3(C≡CPh) and (PNP^{tBu})Re(H)$_4$ were not observed. After 4 days at 22 °C the ratio of (PNP^{tBu})Re(C≡CPh)$_2$, (PNP^{tBu})ReD_3(C≡CPh), and (PNP^{tBu})Re(D)$_4$ was 27:18:55. The intensity of the ^{1}H hydride peaks was <2% of the theoretical value expected for the fully *protio* components. PhCCD was concomitantly observed (no detectable acetylenic ^{1}H signal).

Acknowledgment. This work was supported by the National Science Foundation. We thank Dr. Cristina Cañada Vilalta for facilitating the SQUID measurements.

Supporting Information Available: Full crystallographic information, including cif files, on two determinations, together with DFT optimized geometries on molecules described in the text are available free of charge via the Internet at http://pubs.acs.org.

OM049424I